MEASUREMENT OF HYGROTHERMAL EXPANSION OF ASYMMETRIC COMPOSITE PANELS

Ernest G. Wolff and Darrell W. Oakes
Precision Measurements and Instruments Corporation, Corvallis OR 97333 USA

Keywords: Hygrothermal coefficients, asymmetry, panels, interferometry, curvature, elasticity

Abstract

Hygrothermal coefficients of expansion are important design parameters for large composite panels or structures subjected to significant changes in temperature, humidity or pressure, such as space based solar panels, antennas or optics supports. Such applications require exceptional dimensional stability even with coatings (such as conducting or thermal control films or paints) which generally make them asymmetrical in cross section. Measurement techniques for hygrothermal properties such as linear inplane coefficients of thermal expansion, CTE (α_{11} or α_{22}) or coefficients of moisture expansion, CME (β_{11} or β_{22}) must recognize and quantify out-of-plane distortions to an accuracy of parts per million. This paper outlines a test and analysis approach which gives accurate information on the response of asymmetrical panels to hygrothermal loadings. Laser Michelson interferometry and curvature measurements were made on a metal coated sandwich structure. Representative data demonstrate good agreement with a model based on nonlinear elasticity. It is also shown that the nonlinear terms are especially important for near zero CTE panels. The theory is also extended to related distortions.

1 Introduction

Composite sandwich structures are commonly used for solar panel supports on spacecraft and for antenna reflector or horn structures. In both cases, the overall panel is often midplane asymmetrical. For example, solar panels supports often employ antireflection coatings or paints even before solar panels are bonded to the other side. Antenna structures commonly use both solar reflector coatings and overlays or integral bonded electrical conductors near surfaces. Both uniform and non-uniform temperature or humidity changes will cause bending and/or warping. Consequences include stresses at attachment points leading to detachment of solar cells, electromagnetic field distortions, and pointing and focus errors. The application of polycarbonate (PC) plates in a photovoltaic module design led to warpage after the lamination process due to differences in thermal expansion between solar cells and the PC [1]. Experience has shown that with the need for lighter weight composites (thinner plies and facesheets) and greater performance requirements, coatings and asymmetries of any kind can no longer be ignored.

Intentional causes of asymmetry include not only coatings, films and claddings but also interleaving as a means to prevent crack propagation. Unintentional sources of midplane asymmetry include wrong stacking sequence, extra plies, fabric waviness or wrinkles, variations in ply, core or facesheet stiffness or thickness and/or alignment, and ply slippage before gelation. Problems arise from asymmetry in molding systems, high compression pressures causing tow/fiber/cloth contacts and uneven resin flow from cores to facesheets depending on the assembly or curing process. Dimpling of the facesheet, a common feature with large cell honeycomb structures, not only causes asymmetry but also contributes to attachment and measurement difficulties. Selective microcracking, thermal or stress cycling and non-uniform moisture ab/desorption can cause asymmetry during service.

Classical lamination theory (CLT) cannot by itself predict the shapes of unsymmetrical laminates after cooling from the curing temperature [2-4]. CLT predicts an anti-clastic, hyperbolic paraboloid or saddle shape. It cannot predict the observed cylindrical shapes, which depend on a size effect, nor the snap-through possibility, nor the edge/end effects. For example, if “L” is taken as the laminate side length and “h” its thickness, then the final shape changes from a saddle to a cylinder as L/h increases

beyond a critical value. In order to predict the cured shapes, one needs to extend CLT to take the mechanical and hygrothermal properties of the material into consideration together with fabrication parameters such as cure and stress-free temperatures, dwell time and cooling rate. If we consider the non-linear effects such as slippage between the tool and sample [5,6], the displacement field requires a higher order theory. We must note that while tooling constraints are often present during fabrication cool-down, these are not present during CTE measurements, so that curvature changes during testing will be different from curvatures during fabrication.

The dimensional stability demanded of composite spacecraft components such as metering structures, struts, masts, booms, telescope bezels, etc., translates into very low CTE values and these in turn demand highly precise measurement techniques, such as laser Michelson interferometry [7]. Normally, measurements are accurate if the sample deforms in a simple and/or predictable manner, such as uniform, inplane, linear expansion or contraction. If simultaneous bending or other warping occurs, as with many hygrothermal loadings, measurement techniques must be corrected or modified.

Another reason to correct thermal expansion data for curvature in composite materials technology is the need for accurate dimensional data during thermal cycling. Gradual changes in CTE in polymer and ceramic matrix composites are caused by microcracking, creep and viscoplastic deformations of the matrix. Hysteresis loops in strain-temperature curves are caused by plastic yielding in metal matrix composites. Measurements may be obscured if there is simultaneous deformation due to bending or warping.

Experimental Approach

Laser Michelson interferometry is chosen for linear CTE measurement because of its relative lack of sample contact, accuracy, resolution (to nanometers) and flexibility to take arbitrarily shaped and sized samples [7] (Fig.1). Previous work [8] outlined a procedure for converting changes in fringe amplitude to sample curvature. This was based on rigidly attached mirrors. However, there may be confusion in the interpretation of a small change in fringe amplitude – does it signify a change in overall length or warping? There is also uncertainty of the effects of adhesive bonds or mechanical clamps used to hold the mirrors. Sample constraints to prevent bowing may induce microcracks and cause bending/extensional coupling. A cat's eye reflector is difficult to athermalize if close to the reflecting mirror and ineffective as distance from the mirror increases.

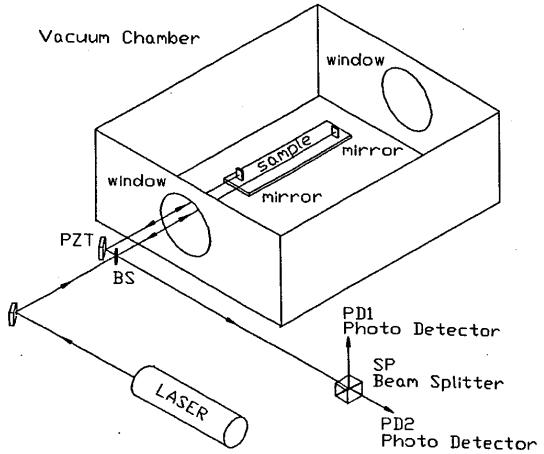

Fig.1 Schematic of a laser based Michelson interferometer for thermal expansion of panels

We have recently improved the blade method [9] (Fig. 2) to maintain the interferometer signal during bowing or warpage. Here a mirror is mounted on a razor blade attached to a quartz rod whose other end is maintained parallel to the (initial) midplane and is free to translate on another quartz roller. When this roller is at the opposite end of the first mirror and next to the second, it keeps the mirrors perpendicular to the initial sample midplane rather than allowing mirror rotation as the sample bends or twists. The laser spots in Fig. 2 are above the sample surface. Their exact position on the mirrors does not matter because their motion is the same as the sample surface, which gives the relative movement of two parallel grooves near the ends of the sample and perpendicular to the length direction.

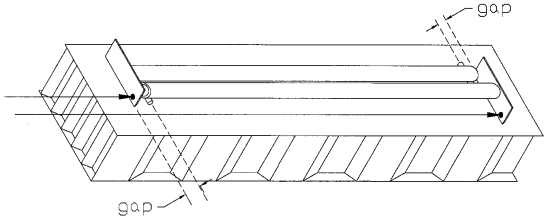

Fig.2 Mounting of interferometer mirrors on a sandwich panel

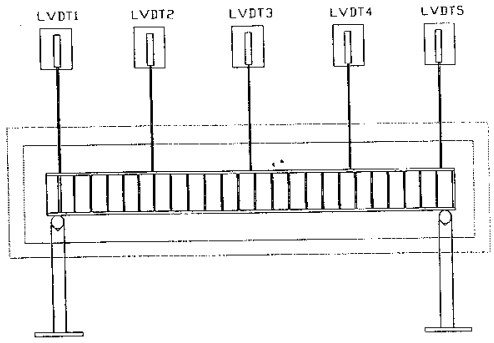

Fig. 3 Use of LVDTs and quartz rod extensions into heater/cooler zone for curvature measurement

Independent measurement of the sample curvature may be accomplished by the use of quartz rods attached to LVDT (linear variable differential transducer) cores, which can be positioned outside the heated/cooled zone for stability (Fig. 3).

Theory

We recall the strain-displacement relations from linear elasticity theory. Let u, v and w be the x, y and z direction displacements. Let the superscript o refer to laminate midplane quantities. The Kirchoff hypothesis allows one to consider the normal to the midplane a straight line whether or not there is sample curvature (thus $w = w^o$). It may be assumed [2,3] that the functional form of w (x, y) is

$$w(x, y) = -\tfrac{1}{2}\,(\kappa_x x^2 + \kappa_y y^2) + \kappa_s xy \qquad (1)$$

The curvature $\kappa_x = 1/R_x = (-\delta^2 w/\delta x^2)$ where R_x is the radius of curvature in the x-z plane, and is infinite for a perfectly flat surface. The measured radius of curvature is $R \pm h/2$ depending on which surface the curvature is measured. We note that if the constants $\kappa_x = 0$, $\kappa_y \neq 0$ or $\kappa_x \neq 0$, $\kappa_y = 0$ we get a cylindrical shape, whereas if $\kappa_x = -\kappa_y$, the classical saddle shape appears. The general equation for measured strain in the x-direction is

$$\varepsilon_x = \delta u^o/\delta x + \tfrac{1}{2}(\delta w/\delta x)^2 \pm z\,(\kappa_x - \kappa_x{}^o) \qquad (2)$$

The second term accounts for nonlinear geometric effects and the third for bending measured away from the midplane. The measurements, especially for asymmetric materials, are not necessarily made along a sample midplane axis (x, y or z). However, the general objective is to derive the basic material property, namely

$$\text{CTE} = \alpha_x = \varepsilon_x{}^o/\delta T = (\delta u^o/\delta x)/\delta T \qquad (3)$$

Figure 4 illustrates the main parameters of a model for half the sample length (L_o). We note that the chosen method of strain measurement follows only displacements along the x' axis, as indicated by motion of the mirror M at point C. We assume that the warped shape is cylindrical, so that the curvature is circular. The x and x' axes originally coincide but diverge during hygrothermal loading. The initial length of the sample is $L_o/2 = OA$. The final length is OB so that the displacement in the x-axis due to hygrothermal loading is AB (or $\pm u^o$). We assume that the thermal displacement continues along the same curvature κ_x as the warping. Thus the measured displacement u is;

$$u = R(\pm\Delta\varphi) - z(\delta w/\delta x) \qquad (4)$$

where z is the distance from the midplane to the mirror M. The angles φ_o and $\Delta\varphi$ are derived from the measured total displacement $\Delta x'$;

$$\Delta x'/2 = Oc' - OA = (R - z)\sin(\varphi_o \pm \Delta\varphi) - L_o/2 \qquad (5)$$

We note that without hygrothermal expansion, OA on the x axis equals OA on the x' axis. Thus for warping only,

$$OA = L_o/2 = R\,\varphi_o \qquad (6)$$

Combining (5) and (6) gives:

$$\pm\Delta\varphi = \sin^{-1}[(\Delta x' + L_o)/2(R - z)] - L_o/2R \qquad (7)$$

Combining equation (2) (except for the nonlinear term) with (4) and (7) gives

$$\varepsilon_x = (2R/L_o)\{\sin^{-1}[(\Delta x' + L_o)/2(R - z)] - L_o/2R\} - z(1/R - 1/R_o) \qquad (8)$$

If bowing is in the reverse direction from that shown in Fig 3, the mirrors will be on the expanded side and the term (R- z) changes to (R + z).

The second term in Eq.2 is normally derived from the difference in length from an element in a

curve to its projected length along the axis of interest [10].

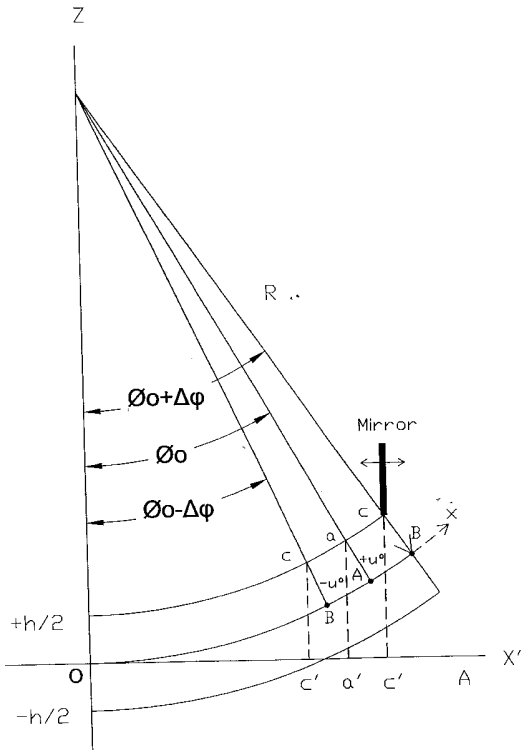

Fig.4 Schematic for analysis of curving panel of thickness h and total initial length = 2 OA

The length of the sample in Fig 4 from the origin to point A on the midplane may be expressed as [11];

$$L_O^A = \int_0^a \left(1 + \left(\partial w / \partial x' \right)^2 \right)^{1/2} dx' \qquad (9)$$

Note that all quantities here are referenced to the original (x') axis). This can be evaluated with help from the binomial expansion for small deflections ($d^2 < c^2$);

$$(c + d)^n = c^n + n\, c^{n-1} d + n(n-1)\, c^{n-2} d^2 / 2! + n(n-1)(n-2)\, c^{n-3} d^3 / 3! + \ldots \qquad (10)$$

Eq. 1 indicates $\partial w/\partial x = -\kappa_x x - \kappa_y y + \kappa_s y$. Thus $(\partial w/\partial x)^2$ at $y = 0$ is $\kappa^2 x^2 = d$ in Eq. 10. We can take $c = 1$, $n = ½$. Using the first three terms in Eq. 10 the length of the arc, referenced to the x'axis, in the absence of thermal expansion, should equal the original length

$$L_o^A = a + \kappa^2 a^3 / 6 - \kappa^4 a^5 / 40 = L_o / 2 \qquad (11)$$

The projected length on the x' axis (0-a) is found by solving for a in Eq. 11. The difference between this and the original length should equal that part of $\Delta x'/2$ due purely to curling. Equivalent expressions are given by Hyer [2, eq. 12] or derivable from equations 4-8 as

$$\Delta x'/2 \text{ (curling only)} = R \sin (L_o/2R) - L_o/2 \qquad (12)$$

The measured deflection due only to curling can also be estimated from the equation for radius of curvature for a bimetallic strip [12]. We can calculate R from;

$$R = h \{3(1 + m)^2 + (1 + mn)[m^2 + (1/mn)]\} / \{ 6 (\alpha_2 - \alpha_1) (T - T_o) (1 + m)^2\} \qquad (13)$$

where side 2 has the higher CTE , m is h_1/h_2 and $n = E_1/E_2$ where E = modulus of elasticity. Combining this with Eq. 12 indicates that the log of $\Delta x'$ increases linearly with the log of the effective change in CTE across the midplane of the sample when the net CTE is zero.

Results

Figures 5 and 6 show typical test results for a sandwich panel (z = h/2 = 12mm) coated on one side with a copper film. Figure 5 shows the thermally induced strain as calculated from $\Delta x'/L_o$. The distance between the mirrors (L_o) was 203 mm on top of the sample. It is seen that $\Delta x' = -0.1039$ mm for a ΔT of –100K when the copper side was down and -0.1516 mm when it was on top. Fig. 6 shows the motions of the sample ends (LVDT#5 and #1) at about 250 mm apart and the sample midplane (LVDT#3) for the setup of Fig. 3. In this case the copper was on the upper side so bowing raised the sample ends on cooling. The ends of the sample move up initially due to bowing and later they move down, presumably due to cooling of the sample supports.

If we compare the vertical deflection of the center (w_c) when the ends are at the same position for a $\Delta T = -100$K we obtain a deflection Δz of 0.076 mm

$$\text{Thus } (R - z) \sim L^2 / (8\, w_c) = 1e5 \text{ mm} \qquad (14)$$

for $\Delta T = 100$K. Application of Eq. 8 to the lower curve of Fig. 5 with $\Delta x' = -0.1516$ mm (for $\Delta T = -100$K) gives a midplane strain ε_x^o of -629

microstrain and a bending contribution of –116 microstrain for a total strain ε_x = -747 microstrain, as measured. A similar analysis with adjustments for R and Z as indicated above was made for the upper curve of Fig. 5, where the copper side is below the sample. For a $\Delta x'$ = -0.1039, ε_x = -512 microstrain, as measured. Again, the calculated midplane strain ε_x^o is –628 microstrain so the true CTE is again 6.28e-6/K.

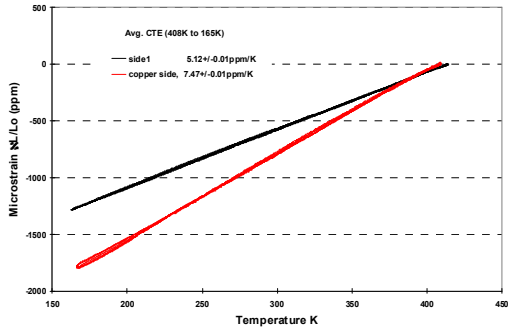

Fig.5 Temperature versus microstrain when (a) uncoated panel side is up (upper curve) and b) copper coated side is up (lower curve)

Use of equations (11) or (12) for these results indicates that $\Delta x'$ measured for curling only is -33 e–6 mm or an equivalent strain of 0.16 ppm. This is negligible here compared to 628 microstrain above, but would be significant for panels with CTE's closer to zero.

Eq. 13 also suggests that a midplane zero CTE panel with $\Delta\alpha$ of 1.5ppm/K (e.g. α_2 = +0.75 ppm/K and α_1 = -0.75 ppm/K) would also result in a $\Delta x'$ of about 31 e-6 mm with an R of 1.07 e5 mm (for h = 24mm). We can assume m ~ n ~ 1 for a midplane symmetrical sandwich plated on one side with Cu.

Discussion

The results indicate that the midplane strain and hence true CTE are derivable from a measurement using either side of the sample, provided one knows the radius of curvature and the direction of bowing. This value is close to the average of the strains measured from separate sides of the sample, provided $\Delta x'$ due to bending alone is negligible. The results also agree with measurements made on a laminate prone to warping on cooling or heating (See Fig 6). In this case the average CTE was obtained by keeping the sample flat with weights. In the present case (a sandwich structure) it would not be possible to flatten the sample without danger of microcracking or other damage. The results also verify the assumption that bowing is uniform and produces a cylindrical shape.

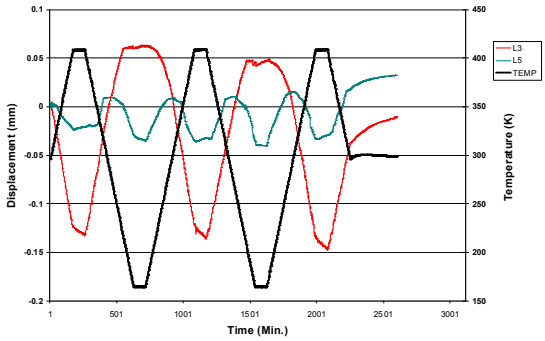

Fig. 6 Displacement versus time and temperature for the upper panel side, measured as shown in Fig. 3. L3 is the midpoint LVDT, L5 is at the supported end point of the panel.

The requirement to know the radius of curvature suggests an additional measurement unless a separate mirror is attached. This might involve a quartz rod (in Fig 2) sitting on a transverse rod at the midpoint of the sample (x = L_o/2). It must indicate both R and the direction of bowing. We note that the change in (R-z), not R alone is measured as in Fig. 3. Thus it can be shown that transverse sample expansion or contraction has a negligible effect on the present results and should be considered only if curvature changes are very small.

We recall from laminate theory that an unsymmetric laminate will always exhibit bending-stretching coupling effects. Bowing occurs because one side has a different CTE than the other. Once bowing occurs, there is an additional inplane displacement due to the coupling effect. This implies that the net midplane shrinkage or extension is due to both thermal and mechanical effects. These effects must be determined analytically by considering the measured inplane strain, the observed changes in curvature, and the composite laminate constants, B_{ij} , (principally B_{11}, B_{22} and B_{12}). [16]. The theory to predict a midplane sandwich CTE , taking into account the core cell size and direction was described in [13,14].

What about sample twisting? A pure twist is where the mirrors rotate only in the z-y plane and remain parallel. This would not be detected. However, rotation in the x-y plane (κ_y) would cause loss of signal and hence even with the blade arrangement, distortions out of the z-x plane would be detected (as outlined in [8] with a quadrature or planar photodetector).

Could the same results occur if only the coated sided bowed – that is the sample distorted rather than bowed uniformly? This would negate the Kirchoff hypothesis and imply h varies with x, so that $\delta w/\delta x$ is not constant. The results above suggest no sample distortion other than simple bowing. In any case, sample distortion is likely to be accompanied by sample damage and thus the CTE results would change with hygrothermal cycling.

Alternative methods to measure total sample distortions include holography, shearography, speckle interferometry, autocollimators, machine vision, and possibly optical levers. In each case there are questions of accuracy, and additionally considerations such as sample translation, sample size and shape, and determination of simultaneous inplane CTE.

Conclusions

The properties of coatings are often difficult to determine but the possibility of accurate simultaneous measurement of inplane CTE and curvature change of asymmetrical composites described here should allow derivation of the coating properties as they contribute to the overall composite behavior. This work has described convenient experimental and analytical methods to determining the true inplane hygrothermal coefficients for unsymmetrical laminates or sandwich structures. It was shown that if the radius of curvature is measured separately, only one expansion test is needed. Unless the CTE (or CME) is close to zero, the correction due to sample warping or curling is negligible.

Acknowledgments

Thanks are due to Hong Chen and Eric Henthorne of PMIC for help with the data analysis and David Stumpff for experimental setup. Thanks are also due to Professor Tim Kennedy of the Mechanical Engineering Department of Oregon State University for valuable discussions.

References

[1] Hackman ,M. M., Meuwissen M.H.H., Bots T.L., Buijs J.A.H.M., Broek K.M., Kinderman R., Tanck O.B.F. and Schuurmans F.M. "Technical Feasibility Study on Polycarbonate Solar Panels" pp105-115, 2004.

[2] Hyer M.W. "The Room-Temperature Shapes of Four-Layer Unsymmetric Cross-Ply Laminates" J. Comp. Mat. Vol. 16 pp318-340, 1982.

[3] Harper B.D. "The Effects of Moisture Induced Swelling Upon the Shapes of Anti-Symmetric Cross-Ply Laminates" J. Comp. Mat. Vol. 21 pp36-48, 1987

[4] Luo J.J. and I.M. Daniel I.M., "Thermally Induced Deformation of Asymmetric Composite Laminates "Proc. of the American Society for Composites., 18th Technical Conference, ASC18, Gainesville, FL, 2003

[5] Cho, M., Kim M-H., Choi H.S., Chung C.H., Ahn K-J., and Eom Y.S. "A Study on the Room-Temperature Curvature Shapes of Un-symmetric (5) pp460-482, 1998

[6] Takatoya T., Chung K., . Wu Y-J., and Seferis J.C., "Evaluation of the Coefficient of Moisture Expansion using Transient Simulated Laminates Methodology (TSL) paper #1135, ICCM-12-Europe, Paris, 1999.

[7] Wolff E.G., "Fundamentals of Optical Interferometry for Thermal Expansion Measurements" "Thermal Conductivity 27/Thermal Expansion 15" DEStech Publications, Inc. Editors H. Wang and W. Porter pp615-633, 2005.

[8] Wolff E.G., "Thermal Expansion of Asymmetrical Laminates" Thermal Conductivity24/Thermal Expansion 12" Ed. Gaal P.,and Apostolescu D.E., Technomic Publ. Co, Lancaster PA pp351-367, 1999

[9] Norris M., Oakes D.W. and Wolff E.G., "Thermal Expansion Measurement of Composite Structures" 40th Intl. SAMPE Symposium, pp1855-1866, May 8-11, 1995

[10] Timoshenko S. and Woinowsky-Krieger S., "*Theory of Plates and Shells*" McGraw Hill Book Company 2nd Edition p 384 1959

[11] G.B. Thomas,G.B., *"Calculus and Analytic Geometry"* Addison-Wesley Press, p185 1951

[12] Eskin S.G. and Fritze J.R.,"Thermostatic Bimetals" Trans ASME Vol 62, pp433-442 1940

[13] Wolff E.G., Chen H., and Oakes D.W., "Hygrothermal Deformation of Composite Sandwich Panels" 12th Intl. Conf. on Composite Materials ICCM-12 Paris 1999

[14] Wolff, E.G. "Intr. to the Dimensional Stability of Composite Materials" DEStech Publ. 2004